A Methodology to Simulate Induction Motor Dynamic Performance in the ABC Reference Frame Considering Mixed Eccentricity Effects

R. Flores-Angeles[*], D. Olguín-Salinas

Escuela Superior de Ingeniería Mecánica y Eléctrica (ESIME)
Instituto Politécnico Nacional
México, D. F., México
*robertf_@msn.com

ABSTRACT

This paper presents a methodology to compute the inductances of the abc induction motor model considering mixed eccentricity. The winding function method (WFM) is employed to calculate the magnetizing inductances. Moreover, the air gap is approximated by an expression which can consider the case mentioned before as well as the healthy case (i.e., with uniform air gap). Due to the fact that the dynamic performance of the machine depends strongly on its inductances, some basic dimensions of a real machine are used and a comparison between different free acceleration characteristics is given such as currents, electromagnetic torque and speed.

Keywords: air-gap distribution, eccentricity, inductance computation, induction motor, winding function method

RESUMEN

En este trabajo se presenta una metodología para el cálculo de las inductancias del motor de inducción considerando su modelo en el marco de referencia abc y bajo condiciones de excentricidad mixta. Se emplea el método de función de devanado (MFD) para calcular las inductancias de magnetización de la máquina. Asimismo, la distribución del entrehierro se aproxima por medio de una expresión la cual puede considerar el caso antes mencionado además del caso sano (i.e., entrehierro uniforme). Debido a que la dinámica de la máquina depende fuertemente de sus inductancias, se muestra la comparación de resultados de un arranque en vacío mostrando variables como corrientes, par electromagnético y velocidad, empleando algunas dimensiones básicas de una máquina real.

1. Introduction

When stator, rotor and rotation axes coincide, it is said that air-gap distribution is uniform; otherwise, a phenomenon called eccentricity is presented [1]. In large motors strict design criteria are established in order to obtain the smallest level of non-uniform air gap; nevertheless, it is not possible to avoid this fault when the machine has been installed. Experts in diagnosis of electric machinery have verified that eccentricity faults mainly appear in machines coupled with their mechanical load [2], [3]. An acceptable level of eccentricity is 10%. However, in the manufacture process this amount is smaller to reduce the resulting vibrations and noise. Besides, an extreme value can cause high levels of vibrations, wear of bearings, friction between stator and rotor and, as a result, the damage of windings and core. A level of 20% is not acceptable and a 50% is a serious problem in which the motor must be repaired [3]. Simulations play an important part in the analysis of electric machinery since healthy and faulty conditions can be computed; afterwards, the results are useful in the laboratory to establish patterns which help diagnose different sorts of failures [4], [5]. In order to perform the dynamic simulation as well as the inductance calculation, it is necessary to get some dimensions and parameters. Hence, a small induction motor was rebuilt to obtain the winding configuration, connections and the rotor mass to determine its inertia. Furthermore, basic electric tests were carried out in the laboratory to obtain the necessary parameters to solve the induction motor state model [6]. With these parameters, dimensions and the abc motor model, a program in Fortran 90 was developed. Different free acceleration characteristics considering both healthy and eccentric cases were obtained, such as currents, electromagnetic torque and speed.

2. Dynamic model of the induction motor in the abc reference frame

The motor model is formulated in the abc reference frame. For this reason there are some inductances that depend on the rotor position and are affected when the air gap is non-uniform. It is important to mention that the squirrel cage is considered as a wound rotor. Taking into account the equations that describe the mechanical behavior, the resulting model is of eighth order as shown in (1) [6], [7]. Where θ_r is the rotor position, ω_r the rotor speed, ψ the flux linkages, P the number of poles, J the rotor inertia, T_e and T_m the electromagnetic and mechanical torque, respectively, $e_{abc,s}$ the terminal voltages and the terms z_{ij} are in function of the resistance and inductance matrices of the windings. The model is represented in flux state variables; therefore, the inverse of the inductance matrix is computed each iteration. Due to this complex process, all the inductances need to be calculated accurately.

$$p\begin{bmatrix} \theta_r \\ \omega_r \\ \psi_{as} \\ \psi_{bs} \\ \psi_{cs} \\ \psi'_{ar} \\ \psi'_{br} \\ \psi'_{cr} \end{bmatrix} = \begin{bmatrix} 0 & 1 & 0 & 0 & 0 & 0 & 0 & 0 \\ 0 & 0 & 0 & 0 & 0 & 0 & 0 & 0 \\ 0 & 0 & z_{11} & z_{12} & z_{13} & z_{14} & z_{15} & z_{16} \\ 0 & 0 & z_{21} & z_{22} & z_{23} & z_{24} & z_{25} & z_{26} \\ 0 & 0 & z_{31} & z_{32} & z_{33} & z_{34} & z_{35} & z_{36} \\ 0 & 0 & z_{41} & z_{42} & z_{43} & z_{44} & z_{45} & z_{46} \\ 0 & 0 & z_{51} & z_{52} & z_{53} & z_{54} & z_{55} & z_{56} \\ 0 & 0 & z_{61} & z_{62} & z_{63} & z_{64} & z_{65} & z_{66} \end{bmatrix} \begin{bmatrix} \theta_r \\ \omega_r \\ \psi_{as} \\ \psi_{bs} \\ \psi_{cs} \\ \psi'_{ar} \\ \psi'_{br} \\ \psi'_{cr} \end{bmatrix} + \begin{bmatrix} 0 \\ \frac{P}{2J}(T_e - T_m) \\ e_{as} \\ e_{bs} \\ e_{cs} \\ 0 \\ 0 \\ 0 \end{bmatrix} \quad (1)$$

3. Winding function method for the inductance calculation under eccentric conditions

3.1 Inductance

The purpose of this method is to determine the radial component of the air-gap magnetic field using cylindrical coordinates [8]-[10]. The winding function represents the mmf across the air gap as a result of a circulating current [4]. The inductance calculation is based on the flux-linkage method and an expression to obtain an inductance between two arbitrary windings x,y is obtained. Equation (2) can be used in non-uniform and healthy conditions [11],[12].

$$L_{yx} = 2\pi\mu_0 rl \left[\langle Pn_x n_y \rangle - \frac{\langle Pn_x \rangle \langle Pn_y \rangle}{\langle P \rangle} \right] \quad (2)$$

Where L_{yx} is the inductance between winding y and x; μ_0 the permeability of the free space; the operator $\langle f \rangle$ is defined as the average value of the function inside; n_x, n_y are the turn functions of windings x and y, respectively; *P* is the distribution of inverse of air gap. The self inductance is computed simply by setting y=x.

3.2 Eccentricity

There are two kinds of eccentricity: static and dynamic; nevertheless, they appear together in real machines [3],[6],[13]. The first case occurs when only the rotation and rotor axes coincide, the minimum air gap is fixed in space and it is not function of the rotor position; the second one happens when the rotor axis rotates around the stator axis. This can be appreciated in Figures 1 and 2, respectively. In the first figure the minimum air gap does not move with rotor position. However, in the second one it can be seen that the minimum air gap changes its position together with the rotor, the rotor rotates around the rotation axis (dotted line). Mixed eccentricity contains certain degree of the two kinds mentioned before and, in this case, none of the axes coincide.
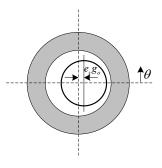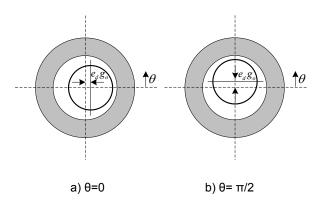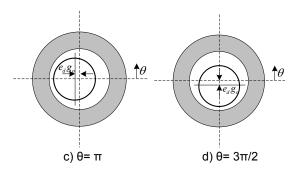

Figure 1. Minimum air gap fixed in space.

a) θ=0   b) θ= π/2

c) θ= π   d) θ= 3π/2

Figure 2. Minimum air gap depends
on rotor position [14].

3.3 Air-gap geometrical representation

There is an important term in Equation 2, the distribution of the inverse of air gap *P*, and it depends on its distribution. A function which represents the complete behavior is (3) [15]; where $g(\theta, \theta_r)$ is the air-gap distribution, g_0 the symmetric air-gap distribution, e_s and e_d are the static and dynamic eccentricity coefficients. In this expression effects caused by the non-uniform air gap can be included taking into account static, dynamic and mixed eccentricities assigning different degrees of failure by means of e_s and e_d (i.e., giving them a percentage, as mentioned in the first section).

These coefficients can be obtained by the rotor run-out measurement [3].

$$g(\theta, \theta_r) = g_0\left(1 - e_s\cos\theta - e_d\cos(\theta - \theta_r)\right) \qquad (3)$$

4. Simulation process and results

In order to perform the inductance calculation as well as the dynamic simulation, a program in Fortran 90 was developed. The main dimensions of a small machine are used [6]. Figure 3 shows the digital simulator flowchart.

4.1 Turns function and inverse of air gap

In order to start the simulation, the program needs some basic data to perform the WFM calculation such as number of poles, number of slots, average radius and length of the stator, effective air gap, eccentricity coefficients and order of harmonics to approximate the functions. At each rotor position the air-gap distribution is calculated by means of (3) and then its inverse is computed to perform the inductance calculation using Equation 2. Since the squirrel cage is considered as a wound rotor the turn functions of the stator are the same as the rotor.
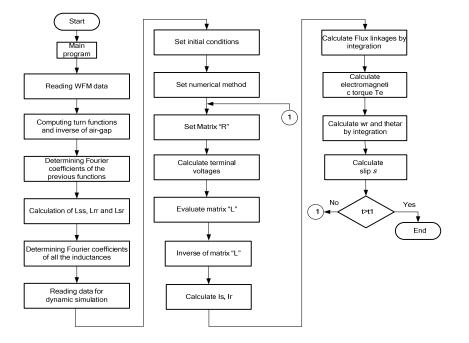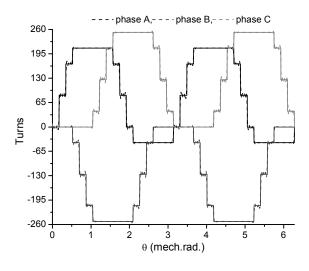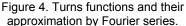

Figure 3. Digital simulator flowchart.

Figure 4 shows the functions by straight lines and also their approximation by Fourier series in dotted lines. These functions represent the number of conductors in each slot considering the direction of the currents passing through them according to the winding configuration. Figure 5 depicts the function of the inverse of air gap for a particular rotor position and for different conditions. The different degrees of eccentricity were chosen arbitrarily in order to show their individual behavior. At this stage the Fourier coefficients of the functions are calculated with the purpose of manipulating them easily [13].
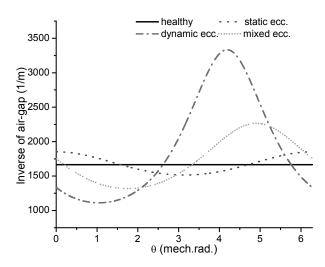
4.2 Machine inductances

With the help of inverse of air gap and turn functions the next step is to calculate the inductances of the state model. Figure 6 shows the stator self and mutual inductances. It can be observed that they are constant and do not depend on rotor position. Also, taking into account the considerations mentioned before, rotor inductances have the same behavior. On the other hand, mutual inductances between stator and rotor vary sinusoidally with rotor position. Figure 7 shows the mutual inductance between stator phase a and rotor windings; phases b and c are the same but displaced 120°. In this case, the Fourier coefficients of the inductances are useful to consider the rotor position inside the transient simulation [13].
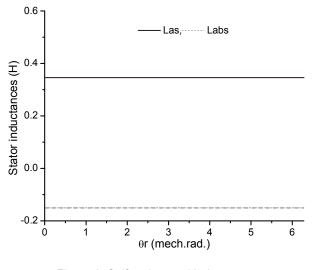

Figure 4. Turns functions and their approximation by Fourier series.

Figure 6. Self and mutual inductances of the stator windings.

Figure 5. Inverse of air gap. Rotor position: θ_r=240°.

When mixed eccentricity effects are considered, the inductances of both stator and rotor are modified and vary respect to rotor position due to the fact that not any axes coincide and the permeance is variable. The inductances behavior is similar in stator and rotor windings, however, their mutual inductances have a changing amplitude depending on the percentage of the total eccentricity. Figure 8 shows the stator self inductances. It can be seen that a big distortion occurs when the fault level is bigger. Also, the affectation due to 30% statics and 30% dynamics differs from 50% statics and 10% dynamics, this implies that this effect is related not

only to the total percentage but also to the contribution of each kind of eccentricity. Figure 9 depicts the mutual inductance between windings of stator phase a and rotor windings. The percentages used in this analysis were chosen to demonstrate that more than 50% cause more distortion to the inductances than the percentages close to the healthy case, such as 20%.
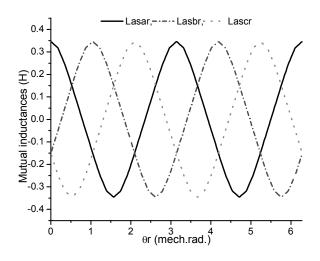

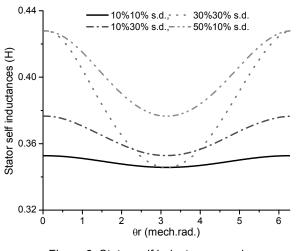Figure 7. Mutual inductances between stator and rotor windings

Figure 8. Stator self inductances under mixed eccentricity.

In Figure 9, it is easy to notice that in the middle of the curve the amplitude is less than that at either sides. This is due to the inverse of air-gap behavior which depends on the angular position of eccentricity as well as the combination of the cases

shown in Figure 1 and Figure 2. Besides, despite the fact that the level of eccentricity is the same, they have different effects on the inductance. The affectation is more remarkable when the percentage of each eccentricity is 30%.
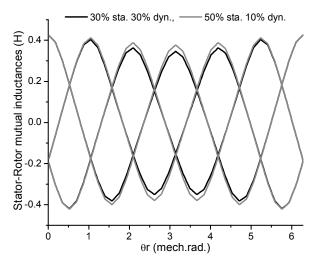

Figure 9. Mutual inductances between stator phase b and rotor windings, under mixed eccentricity.

4.3 Dynamic performance of the induction machine

Once the inductances under mixed eccentricity fault are calculated, the next step is to simulate the dynamic behavior (in this case the free acceleration characteristics). At this stage, some information is required such as machine parameters, rotor inertia, load torque, simulation times and integration step. After setting the initial conditions, matrices R and L are calculated. At this stage, Fourier coefficients are useful to consider a rotor position in the inductance matrix which is computed at each value of θ_r. Besides, the inverse of L is needed to calculate machine currents. In addition, the program calculates flux linkages ω_r and θ_r by integration as well as electromagnetic torque and slip. Since the purpose of this work is to show the effects of mixed eccentricity on the induction motor dynamic behavior, some starting characteristics are shown. In this part the case of 20% of total eccentricity is not considered since its behavior is similar to the healthy case. The percentages of 40% and 60% are bigger than 10% and 20%. A critical behavior is presented in the dynamic performance of the machine when the percentage of total eccentricity is more than 20%. Figure 10 portrays the stator and rotor currents during the

starting transient. It can be seen that eccentricity causes higher peak values and distortion as well.

Figure 11 shows the electromagnetic torque and speed. Torque pulsations are evident, which in turn affect directly the speed. By comparing the different cases, it can be observed that mixed eccentricity modifies the dynamic behavior of the machine by increasing the peaks of the starting current and torque, as well as producing speed pulsations. Moreover, the graphics are not uniform due to the fact that spatial harmonics are considered in the turns functions by means of Fourier coefficients.
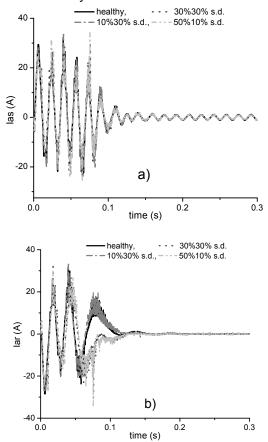

Figure 10. Phase *a* starting current. a) Stator, b) Rotor.

5. Conclusions

Inductance calculation is an important part of the simulation process of the induction machine, even when faults such as eccentricity are considered, since it takes into account non-ideal conditions. Thus, the inductances may be calculated before the

dynamic performance. WFM has been successfully used to calculate machine inductances due to the fact that it is an accurate method which requires just some of the main dimensions. With the help of the air-gap distribution function it can include both healthy and faulty conditions. It has been shown that eccentricity considerably affects the value of inductances by increasing their value and distorting them. Also, constant values become variable, thus modifying the inductance matrix of the motor model. Finally, despite the fact that an abc model is used, eccentricity effects can be taken into account and the variables response have differences between different cases. The mixed eccentricity increases the peak values of the starting current. Also, the electromagnetic torque contains more distortion and pulsations even when the machine reaches its rated speed. The speed is affected by the pulsations in the electromagnetic torque, modifying its characteristic with respect to time.
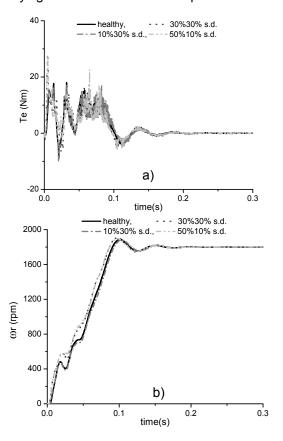

Figure 11. Starting characteristics.
a) Electromagnetic torque, b) Rotor speed.

References

[1] C. Mishra, A. Routray and S. Mukhopadhyay, "Experimental validation of coupled circuit model and simulation of eccentric squirrel cage induction motor," IEEE, pp. 2348-2353, 2006.

[2] J. R. Cameron et al., "Vibration and current monitoring for detecting airgap eccentricity in large induction motors," IEE Proceedings, vol. 133, Pt. B, no. 3, pp. 155-163, May 1986.

[3] W. T. Thomson, "On-line current monitoring and application of a finite element method to predict the level of static airgap eccentricity in three phase induction Motors," IEEE Trans. On Energy Conversion, vol. 13, no. 4, pp. 347-357, December 1998.

[4] H. A. Toliyat et al., "A method for dynamic simulation of air-gap eccentricity in induction machines ," IEEE Trans. on Industry Applications, vol. 32, no.4, pp. 910-918, July/August 1996.

[5] B. Liang et al., "Simulation and fault detection of three-phase induction motors," ELSEVIER, Mathematics and Computers in Simulation, 61 (2002), pp. 1-15, Available: http : // www.elsevier.com/locate/matcom.

[6] R. Flores, "Modelo del motor de inducción incluyendo el efecto de excentricidad," MSc dissertation, Dept. Electrical Engineering, National Polytechnic Institute (IPN), Mexico City., 2011.

[7] R. Flores and D. Olguín, "Comparación de los modelos del motor de inducción en los marcos de referencia dq0 arbitrario y abc", Vigésima Tercera Reunión de Verano de Potencia, Aplicaciones Industriales y Exposición Industrial, Acapulco Guerrero, Mexico, 2010.

[8] N. L. Schmitz and D. W. Novotny, "Introductory Electromechanics", New York: The Ronald Press Company, 1965.

[9] J.J. Grainger and W. D. Stevenson, "Análisis de Sistemas de Potencia", México: Mc. Graw Hill,2007.

[10] X. Luo et al., "Multiple coupled circuit modeling of induction machines," IEEE, Trans. on Industry Applications, vol. 1, pp. 203-210, October 1993.

[11] J. Faiz and I. Tabatabaei, "Extension of winding function theory for nonuniform air gap in electric machinery," IEEE Trans. on Magnetics, vol. 38, no. 6, pp. 3654-3657,November 2002.

[12] R. Flores and D. Olguín, "Método de función de devanado para el cálculo de las inductancias del motor de inducción con rotor jaula de ardilla", presented at XII Congreso Nacional de Ingeniería Electromecánica y de Sistemas, México D.F., 2010.

[13] J. H. Cerón, "Efectos de la Excentricidad en la Estabilidad Transitoria de la Máquina Síncrona de Polos Salientes," MSc dissertation, Dept. Electrical Engineering, National Polytechnic Institute (IPN), Mexico City, 2010.

[14] G. M. Joksimovic et al., "Dynamic simulation of dynamic eccentricity in induction machines- winding function approach," IEEE Trans. On energy conversion, vol.15, no.2, pp. 143-148, June 2000.

[15] G. Bossio et al., "A model for induction motors with non-uniform air-gap," Latin American Applied Research, vol. 35, no. 2 pp. 77-82, 2005.